

Research article

Impact of intravenously administered cranial bone-derived mesenchymal stem cells on functional recovery in experimental spinal cord injury

Kiyoharu Shimizu^{a,*}, Takafumi Mitsuhashi^a, Yuyo Maeda^a, Masashi Kuwabara^a,
Masahiro Hosogai^a, Masaaki Takeda^a, Louis Yuge^b, Nobutaka Horie^a

^a Department of Neurosurgery, Graduate School of Biomedical and Health Sciences, Hiroshima University, Hiroshima, Japan

^b Division of Bio-Environmental Adaptation Sciences, Graduate School of Biomedical and Health Sciences, Hiroshima University, Hiroshima, Japan

ARTICLE INFO

Keywords:

Bone marrow-derived mesenchymal stem cell
Cranial bone marrow
RNA sequencing
Anti-inflammatory
Cervical spinal cord injury

ABSTRACT

Impairments of the central nervous system, such as stroke, brain trauma, and spinal cord injury (SCI), cannot be reversed using current treatment options. Herein, we compared the characteristics of rat cranial bone-derived mesenchymal stem cells (rcMSCs) and rat bone marrow-derived mesenchymal stem cells (rbMSCs). We also investigated the therapeutic effects of intravenously administered rcMSCs and rbMSCs in a rat model of cervical SCI (cSCI) and elucidated its underlying mechanism. Comprehensive comparative bioinformatics analysis of rcMSCs and rbMSCs RNA sequencing revealed that genes associated with leukocyte transendothelial migration and chemokine signaling were significantly downregulated in rcMSCs. Rats were divided into three groups that received intravenous administration of rcMSC, rbMSC, or phosphate-buffered saline (control) 24 h after cSCI. The rcMSC-treated group showed improved functional recovery over the rbMSC-treated and control groups, and reduced lesion volume compared with the control group. The mRNA expression of nitric oxide synthase 2 at the spinal cord lesion site was significantly higher in the rcMSC-treated group than in the control and rbMSCs-treated groups, whereas that of transforming growth factor- β was significantly higher in the rcMSC-treated group compared to that in the control group. The transcriptome data indicated that rcMSCs and rbMSCs differentially affect inflammation. The intravenous administration of rcMSCs contributed to functional recovery and lesion reduction in cSCI. The rcMSCs have the potential to induce an anti-inflammatory environment in cSCI.

1. Introduction

Central nervous system (CNS) disorders, such as stroke, brain trauma, and spinal cord injury (SCI), cause functional impairments that current treatments cannot restore. Cell-based therapy using resources, such as mesenchymal stem cells (MSCs), has attracted attention as a novel approach to treat CNS disorders. We previously succeeded in establishing MSCs from cranial bones, identified as good candidates for CNS therapy because of their neuroprotective properties [1]. Cranial bones are derived from neural crest cells, likely the origin of their neuroprotective potential. This notion is supported by a previous study

indicating that dental pulp-derived MSCs, also derived from neural stem cells, exhibit more prominent neurogenic activity than MSCs from other sources [2]. Our previous study comparing cranial bone-derived and bone marrow-derived MSCs demonstrated that cranial bone-derived MSCs have high anti-inflammatory and anti-apoptotic effects, which are attributed to their neuroprotective properties [3]. An inflammatory response is critical in the secondary injury cascade after CNS injury. Thus, the anti-inflammatory potential of cranial bone-derived MSCs may be more beneficial in treating CNS disorders.

Therefore, we investigated the anti-inflammatory effects of cranial bone-derived MSCs compared with those of bone marrow-derived MSCs

Abbreviations: Actb, β -Actin; CNS, central nervous system; cSCI, cervical spinal cord injury; DEGs, differentially expressed genes; FITC, fluorescein isothiocyanate; GO, Gene Ontology; H&E, hematoxylin and eosin; IL-6, Interleukin-6; IL-10, Interleukin-10; KEGG, Kyoto Encyclopedia of Genes and Genomes; MSCs, mesenchymal stem cells; NO, nitric oxide; NOS2, Nitric oxide synthase 2; PBS, phosphate-buffered saline; PE, phycoerythrin; rbMSCs, rat bone marrow-derived mesenchymal stem cells; rcMSCs, rat cranial bone-derived mesenchymal stem cells; RT-PCR, real-time polymerase chain reactions; SCI, spinal cord injury; TGF- β , transforming growth factor beta; TNF- α , tumor necrosis factor alpha; VEGF, vascular endothelial growth factor.

* Corresponding author at: Department of Neurosurgery, Graduate School of Biomedical and Health Sciences, Hiroshima University, 1-2-3 Kasumi, Minami-ku, Hiroshima-city, Hiroshima 734-8551, Japan.

E-mail address: shimizu.kiyoharu@gmail.com (K. Shimizu).

<https://doi.org/10.1016/j.neulet.2023.137103>

Received 27 December 2022; Received in revised form 21 January 2023; Accepted 30 January 2023

Available online 2 February 2023

0304-3940/© 2023 Elsevier B.V. All rights reserved.

in SCI. Most animal studies use a thoracic SCI model. However, cervical SCI (cSCI) is more prevalent than thoracic SCI in the real world and causes devastating results. Thus, we used a rat model of cSCI to investigate the therapeutic effects of intravenously administered rat cranial bone-derived MSCs (rcMSCs) and rat bone marrow-derived MSCs (rbMSCs) on the functional recovery of cSCI model rats and elucidated its underlying mechanisms.

2. Material and methods

2.1. Ethics statement

All methods have been reported following the Animal Research: Reporting of In Vivo Experiments guidelines (<https://arriveguidelines.org>) and the American Veterinary Medical Association Guidelines for the Euthanasia of Animals (2020). All study protocols were approved by the Animal Testing Committee Guidelines of Hiroshima University (A19-78).

2.2. Isolation and culture of rcMSCs and rbMSCs

The rcMSCs and rbMSCs were isolated and cultured as previously described [3]. Briefly, rcMSCs were isolated from the cranial bone, whereas rbMSCs were isolated from the femur and tibia bone marrow, of 4–5-week-old female Sprague–Dawley (SD) rats weighing 250–300 g. The cranial bone and bone marrow samples were seeded in culture dishes. The adherent cells were detached 7–14 days after sample seeding and collected as rcMSCs and rbMSCs. The dishes were incubated at 37 °C under 5 % CO₂ and the culture medium was changed every 3 days. The collected rcMSCs and rbMSCs were passaged three times at >80 % confluence.

2.3. Flow cytometry analysis for MSC-specific markers

The rcMSCs and rbMSCs at passage 3 were collected using TrypLE™ Select (Thermo Fisher Scientific), and resuspended in phosphate-buffered saline (PBS). Aliquots containing 1.0×10^5 cells were incubated with phycoerythrin (PE) or fluorescein isothiocyanate (FITC)-conjugated antibodies against rat CD45, CD90, CD29 (BD Biosciences, San Jose, CA), CD44 (Biolegend Co., San Diego, CA), and CD34 (Santa Cruz Biotechnology, Dallas, TX). PE-conjugated antibodies against CD29 and CD90 and FITC-conjugated antibodies against CD44 were used as MSC markers, and PE-conjugated antibodies against CD34 and FITC-conjugated antibodies against CD45 were used as hematopoietic markers. PE mouse IgG1 and FITC mouse IgG1 (Biolegend) were used as isotype controls. Data acquisition and analyses were performed using FACS-Verse (BD Biosciences).

2.4. RNA analyses of rcMSC and rbMSC

2.4.1. RNA extraction and quality control

The rcMSCs and rbMSCs at passage three were collected using TrypLE™ Select (Thermo Fisher Scientific). Total RNA was extracted using the NucleoSpin™ RNA mini kit (MACHEREY-NAGEL GmbH & Co. KG, Duren, Germany) following the manufacturer's protocol. The quality of the total RNA was assessed using a Bioanalyzer instrument (Agilent Technologies, Santa Clara, CA, USA) to ensure that the RNA integrity number was >7.0. After poly (A) + RNA enrichment using the NEBNext Poly (A) mRNA Magnetic Isolation Module (New England Biolabs Inc., Ipswich, MA, USA), double-stranded cDNA libraries (RNA-seq libraries) were prepared using the SMARTer Stranded Total RNA Sample Prep Kit – HI Mammalian (Clontech Laboratories, Mountain View, CA, USA) and MGIEasy Universal Library Conversion Kit (App-A; MGI Tech Co., Ltd., Wuhan, China), following the manufacturers' instructions.

2.4.2. RNA library building and sequencing.

RNA-seq libraries were sequenced using paired-end reads (150 nt of reads 1 and 2) on a DNBSEQ-G400RS instrument (MGI Tech Co., Ltd.). The obtained raw reads were trimmed and quality-filtered using the Trim Galore! (version 0.6.7) and Trimmomatic (version 0.39) tools. The trimmed reads were then mapped to the Rat mRatBN7.2 genome using STAR (version 2.7.9a) software. Reads of the annotated genes were counted using the featureCounts program in the “subReads” package (version 2.0.1) in R software.

2.4.3. Analysis of differentially expressed genes between rcMSCs and rbMSCs

Fragments per kilobase million values were calculated from the mapped reads by normalizing them to total counts and transcripts. Differentially expressed genes (DEGs) between rcMSCs and rbMSCs were detected using the “DESeq2” package (version 1.20.0) in R software. The thresholds of significant DEGs were set at $|\log_2\text{fold-change (FC)}| > 1.5$ and $p < 0.05$. Significant DEGs corresponding to $\log_2\text{FC} > 1.5$ and $\log_2\text{FC} < -1.5$ was categorized as upregulated and downregulated DEGs, respectively. DEGs were bar plotted using BioVinci (Biotechnology, San Diego, CA, USA).

2.4.4. Gene Ontology terms and Kyoto Encyclopedia of Genes and Genomes pathways enrichment analyses

Gene Ontology (GO) terms and Kyoto Encyclopedia of Genes and Genomes (KEGG) pathways enrichment analyses were performed using the iDEP (version 0.96) tool (<https://bioinformatics.sdstate.edu/idp96/>). The GO enrichment analysis included three domains: biological processes, cellular components, and molecular functions. KEGG pathway enrichment analysis was performed using the parametric gene set enrichment analysis method. Statistical significance was defined as a $p < 0.05$.

2.5. C5 hemiconfusion SCI model and cell transplantation

The surgical procedure for C5 hemiconfusion SCI was performed on 45 adult female SD rats weighing 250–300 g under isoflurane anesthesia, as previously described [4]. Briefly, a midline dorsal skin incision was made, the paravertebral muscles of C4–6 were detached from the laminae, and a laminectomy was performed at C5. The spinal cord was aligned under a 0.8-mm impactor tip and adjusted to be confined to the left side. Hemiconfusion SCI was induced using an Infinite Horizon impactor (Precision Systems and Instrumentation, Lexington, KY, USA) with an intended force of 100 kdyn. Following cSCI, the musculature and skin were sutured to close the lesion. The analgesia buprenorphine was injected subcutaneously every 12 h, and the antibiotic Penicillin G was injected intramuscularly every 24 h for 3 days.

The rats were divided into three groups following the type of cell transplantation: rcMSC (n = 15), rbMSC (n = 15), and control (n = 15). Confluent cultured rcMSCs and rbMSCs at passage three were collected for transplantation. Rats in the rcMSC and rbMSC groups were injected with MSCs (1.0×10^6 cells in 300 μL PBS via the tail vein 24 h after undergoing cSCI, whereas those in the control group were administered with PBS alone.

2.6. Behavioral testing

Behavioral testing was performed 1, 4, 7, 14, 21, and 28 days after cSCI in the open field. The functional recovery of each fore- and hindlimb ipsilateral to the cSCI was evaluated with 20-point scoring system based on six factors, i.e., fore- and hindlimb articular movement, weight support, digit position, stepping, fore- and hindlimb coordination, and tail position [5].

The motor functions were evaluated by an observer blinded to the group identities. Based on this scoring system, all rats used for motor function evaluation had a total score of 0 for the forelimb and 2 for the

hindlimb at the time of cSCI.

2.7. Morphological assessment of the spinal cord lesion

Twenty-eight days after transplantation, a 1-cm-long spinal cord segment was symmetrically separated at the primary site and embedded in paraffin. The spinal cord was cut into 30- μ m transverse sections every 1 mm over a distance of 6 mm. The segments were mounted on microscope slides for hematoxylin and eosin (H&E) staining and examined using a BZ-9000 fluorescence microscope (Keyence Corp., Osaka, Japan), and cavity areas were quantified using ImageJ software (version 1.53; National Institutes of Health, Bethesda, MD, USA) as described in our previous study [4]. The cavity ratio was calculated for each segment, dividing the cavity area by the total tissue area. All cavity ratios were evaluated by an observer blinded to the group identities.

2.8. Spinal cord lesion mRNA analysis

Seven days after transplantation, four samples of a 5-mm-long spinal cord segment at the primary site of injury site were removed from each group, and total RNA was extracted using the ISOGEN RNA Extraction Kit (Nippon Gene, Tokyo, Japan). Reverse transcription was performed using the ReverTra Ace- α kit (Toyobo Co. Ltd., Osaka, Japan). Real-time polymerase chain reactions (RT-PCR) analyses were performed on the 7900 HT RT-PCR system (Applied Biosystems, Carlsbad, CA, USA) using cDNA as the template with Fast Start Universal Probe Master Mix (Roche, Basel, Switzerland) and TaqMan Gene Expression Assays for rat transforming growth factor beta (TGF- β), interleukin-6 (IL-6), vascular endothelial growth factor (VEGF), tumor necrosis factor- α (TNF- α), nitric oxide synthase 2 (NOS2), and interleukin-10 (IL-10) (Life Technologies, Carlsbad, CA, USA). β -Actin (Actb) was used as an internal endogenous control. The assay IDs for the TaqMan Gene Expression Assays used in this study are listed in Supplementary Table S1. Three

technical replicates of each PCR were performed.

2.9. Statistical analysis

All statistical inferences were performed using a two-sided test at the 5 % significance level. All analyses were performed using the “rms” package in R software version 4.2.0 (<https://cran.r-project.org/>). Student’s *t*-test or Fisher’s exact test was used to assess univariate differences between the groups for continuous or categorical variables, as appropriate. One-way analysis of variance with Tukey’s correction was used for multiple comparisons. Mixed-effects models were used to assess the longitudinal change in fore- and hindlimb functional recovery and serial changes in the lesion cavity ratio in the cephalocaudal direction.

3. Results

3.1. Cell surface marker expression in MSCs

MSC-specific markers in rcMSCs and rbMSCs were analyzed using flow cytometry (Supplementary Table S2). Both rcMSCs and rbMSCs were strongly positive for MSC-specific cell surface markers of CD29, CD90, and CD44, and were intensely negative for hematopoietic-specific cell surface markers, CD34 and CD45.

3.2. Identification and characterization of DEGs between rcMSCs and rbMSCs

Comparative gene expression analysis between rcMSCs and rbMSCs revealed a total of 227 and 191 genes with a 1.5-fold or higher increase and decrease in gene expression, respectively, in rcMSCs compared to rbMSCs (Fig. 1). The GO term enrichment analysis revealed that among biological processes, DEGs implicated in blood vessel development and morphogenesis, cell migration, and regulation of cell migration were

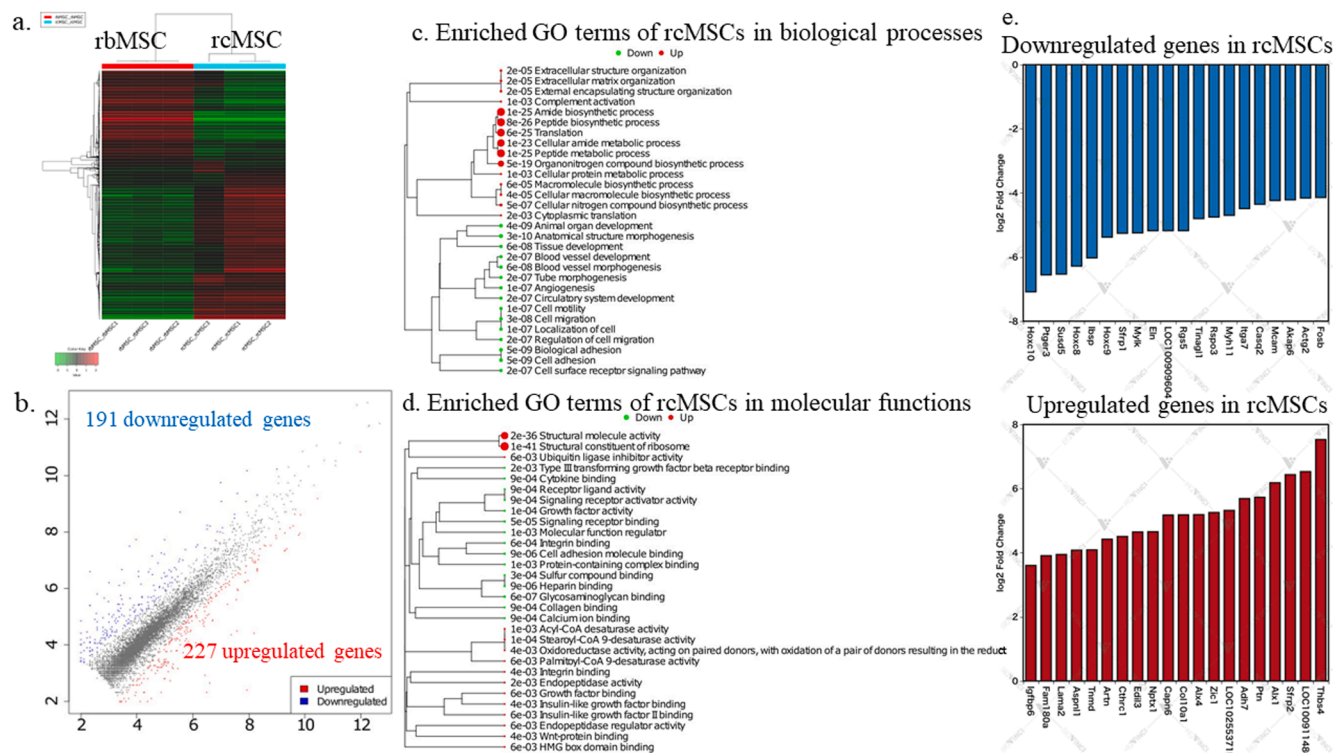


Fig. 1. Differentially expressed genes (DEGs) between rat cranial bone-derived mesenchymal stem cells (rcMSCs) and rat bone marrow-derived mesenchymal stem cells (rbMSCs). (a) Hierarchical clustering and the corresponding heat map. (b) RNA-seq analysis identified 227 and 191 significantly upregulated and downregulated DEGs in rcMSCs, respectively. (c, d) Enriched Gene Ontology (GO) terms of rcMSCs in (c) biological processes and (d) molecular functions. The size of the circle indicated the magnitude of the difference. (e) Most enriched and depleted genes in rcMSCs.

significantly downregulated in rcMSCs. Among molecular functions, DEGs associated with insulin-like growth factor (IGF) and IGF2 binding were significantly upregulated in rcMSCs, whereas those related to cytokine binding were significantly downregulated. The most substantially upregulated DEGs in rcMSCs were THBS4, ALX1, ZIC1, ALX4, and IGFBP6, whereas the most notable downregulated genes were HOX genes, including HOXC10, HOXC8, and HOXC9. KEGG analysis revealed a significant suppression of pathways related to leukocyte transendothelial migration and chemokine signaling in rcMSCs (Fig. 2). Among genes associated with the chemokine signaling pathway, CCL20 and CXCL14 were significantly upregulated, whereas CXCL12, CXCL2, CCL3, CCL2, and CXCR4 were significantly downregulated in rcMSCs.

3.3. Fore- and hindlimb function recovery in cSCI model rats

The improvements in forelimb total scores were significantly more prominent in the rcMSC and rbMSC groups than in the control group on days 4, 7, 14, 21, and 28 after injury ($p < 0.01$, Fig. 3a). The improvement in hindlimb total scores were also significantly more prominent in the rcMSC and rbMSC groups than in the control group on days 4, 7, 14, 21 ($p < 0.01$, Fig. 3b), and 28 after injury ($p < 0.01$, and $p < 0.05$ in the rcMSCs and rbMSC groups, respectively; Fig. 3b). Furthermore, the improvement in forelimb total scores was significantly more prominent in the rcMSC group than in the rbMSC group on days 21 ($p < 0.05$, Fig. 3a) and 28 after injury ($p < 0.01$, Fig. 3a). The improvement in hindlimb total scores was significantly more prominent in the rcMSC group than in the rbMSC group on days 14 ($p < 0.05$, Fig. 3b), 21 ($p < 0.05$, Fig. 3b), and 28 after injury ($p < 0.05$, Fig. 3b). The rcMSC and rbMSC group showed a faster recovery of weight support and articular movements of the affected limbs than that of the control group within the first two weeks. The rcMSC group exhibited a more prominent recovery of anteroposterior coordination than the rbMSC group during the last two weeks of the 28-day recovery period after injury.

3.4. Lesion volumes in cSCI model rats

The cavity ratio was assessed as a measure of spinal cord lesion volume to compare the efficacy of the transplanted rcMSCs and rbMSCs (Supplementary Fig. S1). The cavity ratio at the epicenter of the lesion was significantly smaller in the rcMSC group than in the control group ($p < 0.05$). The cavity ratio of each segment in the cephalocaudal direction was significantly different only between the rcMSC and control group, being significantly smaller in the rcMSC group ($p < 0.01$ for all sections).

3.5. mRNA expression at cSCI lesion site on day 7

The mRNA expression levels of TGF- β , IL-6, VEGF, TNF- α , NOS2, and IL-10 were analyzed at the lesion site 7 days after cSCI to evaluate the anti-inflammatory effects of rcMSCs and rbMSCs (Fig. 4). TGF- β mRNA expression was significantly higher in the rcMSC group than in the control groups ($p < 0.05$). TNF- α mRNA expression was significantly higher in the rcMSC ($p < 0.05$) and rbMSC ($p < 0.01$) groups than in the control group. NOS2 mRNA expression was significantly higher in the rcMSC group than in the rbMSC ($p < 0.05$) and control groups ($p < 0.01$).

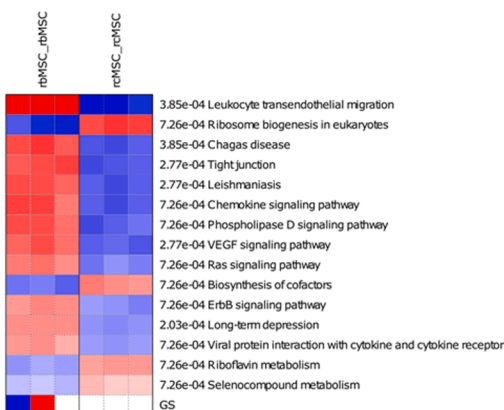
4. Discussion

RNA sequencing results suggested that rcMSCs have the potential to inhibit neutrophil migration and suppress chemokines. The intravenous administration of rcMSCs contributed to functional recovery and lesion reduction in cSCI. Additionally, the expression of NOS2 and TGF- β genes was significantly upregulated in cSCI areas intravenously administered with rcMSCs.

Genome-wide gene expression profiling revealed distinctive differences between rcMSCs and rbMSCs. The present study revealed that the expression of neural crest-associated genes, including ALX1, ALX4, and ZIC1, was higher in rcMSCs than in rbMSCs. The ALX family is highly enriched in neural crest cells and crucial for chondrocyte development [6]. ZIC1 is essential for the initiation of neural crest differentiation and is expressed before FOXD3 and SLUG. In contrast, the expression of HOX family members, including HOXC8, 9, and 10, was significantly lower in rcMSCs than in rbMSCs. HOX is essential for mesodermal patterning and well-described in the vertebrate skeleton [7]. Therefore, the upregulation of HOX genes in rbMSCs is consistent with rbMSCs being derived from the mesodermal germ layer. The most highly expressed gene in the rcMSCs was THBS4, which encodes a protein produced by astrocytes generated in the subventricular zone [8]. In addition, the IGF binding function and its related gene, IGFBP6, were significantly upregulated in rcMSCs. These THBS4 and IGFBP6 act as neuroprotective agents [8,9]. These findings indicated the distinctive profiles of rcMSCs and rbMSCs based on their origin. Thus, rcMSCs may have a neuroprotective advantage over rbMSCs because they are derived from cranial neural crest cells.

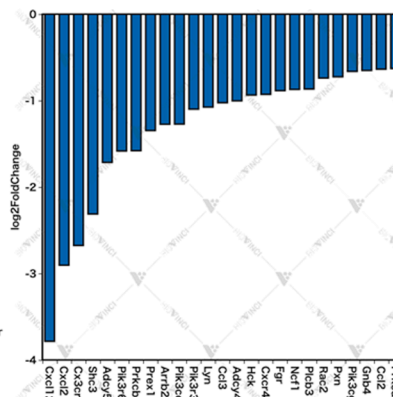
Functional pathway analysis indicated that genes associated with leukocyte transendothelial migration and chemokine signaling pathways were significantly downregulated in rcMSCs. Neutrophil infiltration into the lesion site is the principal response that initiates the

a. Heatmap of enriched pathways



b. DEGs related to the chemokine signaling pathway in rcMSCs

Downregulated genes in rcMSCs



Upregulated genes in rcMSCs

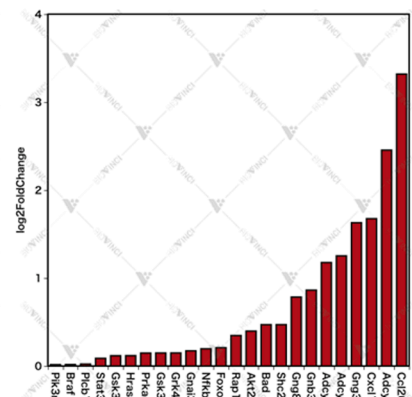


Fig. 2. Kyoto Encyclopedia of Genes and Genomes (KEGG) pathways enrichment analysis of rat cranial bone-derived mesenchymal stem cells (rcMSCs). (a) Heatmap of enriched pathways in rcMSCs. (b) Differentially expressed genes (DEGs) related to the chemokine signaling pathway in rcMSCs.

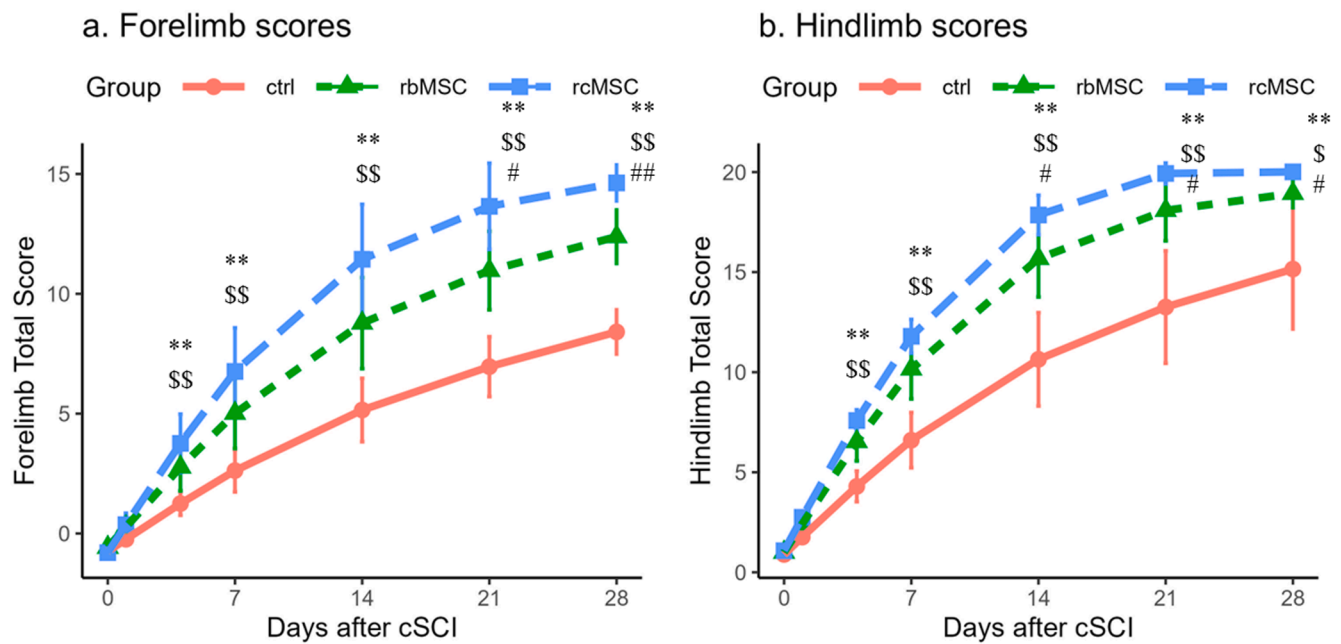


Fig. 3. Longitudinal changes in the scores of affected (a) fore- and (b) hindlimb after cSCI (n = 5). *rcMSC versus the control group, \$rbMSC versus the control group, and #rcMSC versus the rbMSC group (*p < 0.05, **p < 0.01, \$p < 0.05, \$\$p < 0.01, #p < 0.05, and ##p < 0.01). cSCI, cervical spinal cord injury; ctrl, control; rbMSCs, rat bone marrow-derived mesenchymal stem cells; and rcMSCs, rat cranial bone-derived mesenchymal stem cells.

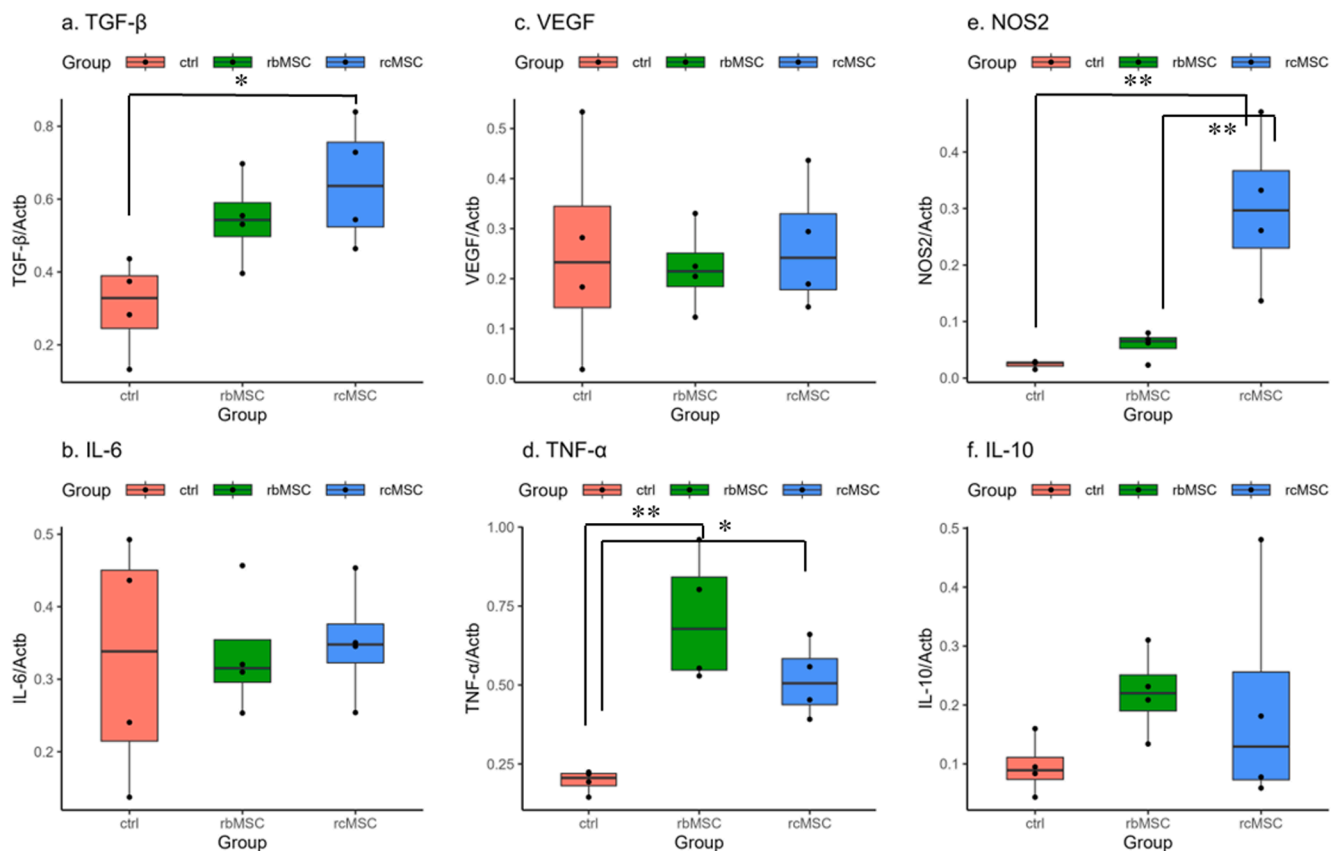


Fig. 4. Mrna expression in the spinal cord injury site 7 days after transplantation (n = 4). Relative mRNA expression of (a) transforming growth factor beta (TGF- β), (b) interleukin-6 (IL-6), (c) vascular endothelial growth factor (VEGF), (d) tumor necrosis factor-alpha (TNF- α), (e) nitric oxide synthase 2 (NOS2), and (f) IL-10, normalized to that of β -actin. *p < 0.05, and **p < 0.01. ctrl, control; rbMSCs, rat bone marrow-derived mesenchymal stem cells; rcMSCs, rat cranial bone-derived mesenchymal stem cells; and Actb, β -actin.

inflammatory response in SCI, which reaches its peak at about 24 h post-SCI [10]. Therefore, inhibiting neutrophil migration to the lesion site is crucial in suppressing inflammation. In addition, the expression of genes associated with the chemokine signaling pathway was significantly downregulated in rcMSCs. This result concurred with a previous report showing that neural crest stem cells are less enriched in chemokines [11]. CXCL12-CXCR4 signaling is essential for maintaining the hematopoietic stem cell pool in the microenvironment niche of the bone marrow, therefore high CXCL12 expression in rbMSCs is mandatory [11]. CCL2 is pro-inflammatory and enhances the migration of macrophages and T cells [11]. Therefore, the low CCL2 expression in rcMSCs is consistent with the leukocyte migration pathway being suppressed by rcMSC. However, CXCL14 expression was significantly upregulated in rcMSCs. CXCL14 is conserved in all classes of vertebrates and considered a primitive chemokine owing to its homeostatic role. Meanwhile, CXCL14 is a potent trophic factor contributing to the high regenerative potential of dental pulp-derived MSCs [2]. These results suggest that the anti-inflammatory effects of rcMSCs are different from those of rbMSCs.

NOS, which catalyzes nitric oxide (NO) production, has three isoforms: inducible NOS (NOS2), neuronal NOS, and endothelial NOS [12]. NO concentrations and NOS activity peak twice after SCI, immediately after SCI (<30 min), and between 24 h and several days after SCI. NOS2 is activated during the late phase after SCI and mediates the anti-inflammatory mechanism leading to tissue-protective effects and improved functional recovery [12]. The MSCs promote NOS2 expression, which requires proinflammatory cytokines such as interferon- γ and TNF- α as triggers [12]. Our study showed high expression of NOS2 along with high expression of TNF α in rcMSCs, supporting the result of above mentioned study. Additionally, rcMSCs had higher mRNA expression of TGF- β , an immunosuppressive factor of MSCs [12]. TGF- β can counteract and downregulate inflammatory and cytotoxic reactions. These results may indicate that rcMSCs induce an anti-inflammatory environment in spinal cord injured tissues mediated by NOS2 and TGF β .

However, this study has certain limitation primarily due to a relatively small number of samples. The lack of significant differences between rcMSCs and rbMSCs may be due to the small sample size. In addition, the DEGs obtained in RNA-seq transcriptome analysis have not been validated using RT-PCR analysis. DEGs between rcMSCs and rbMSCs exposed to inflammatory stress were not analyzed. A direct cause-and-effect relationship between the anti-inflammatory effects under rcMSCs and the anti-inflammatory environment in SCI has not been proved. The improved functional recovery in the rcMSC group may result from a more prolonged survival of rcMSCs after transplantation than rbMSCs, thereby delaying the inflammatory response under rcMSC treatment. However, limited studies have performed a comprehensive RNA expression analysis of cranial bone-derived MSCs, and our results support the utility of cranial bone-derived MSCs in regenerative medicine for treating CNS disorders. Further studies are required to establish the differences in the therapeutic potential of cranial bone-derived and bone marrow-derived MSCs in regenerative medicine.

5. Conclusion

The transcriptome data presented here indicate that rcMSCs and rbMSCs exert differential effects on inflammation. The intravenous administration of rcMSCs contributed to functional recovery and lesion reduction in cSCI. The rcMSCs have the potential to induce an anti-inflammatory environment in cSCI.

Declaration of Competing Interest

The authors declare that they have no known competing financial interests or personal relationships that could have appeared to influence the work reported in this paper.

Data availability

Data will be made available on request.

Acknowledgements

Part of this work was conducted at the Analysis Center of Life Science, Natural Science Center for Basic Research and Development, Hiroshima University. RNA sequence library preparation, sequencing, mapping, gene expression analysis, and GO enrichment analysis using the “clusterProfiler” package in R software were performed by DNA-FORM (Yokohama, Kanagawa, Japan).

Funding

This work was partially supported by a grant-in-aid for Scientific Research from the Japanese Society for the Promotion of Science (JAPS KAKENHI grant no. 18K16561) and by TWO CELLS Co., Ltd., Hiroshima, Japan.

Appendix A. Supplementary data

Supplementary data to this article can be found online at <https://doi.org/10.1016/j.neulet.2023.137103>.

References

- [1] K. Shinagawa, T. Mitsuhashi, T. Okazaki, M. Takeda, S. Yamaguchi, T. Magaki, Y. Okura, H. Uwatoke, Y. Kawahara, L. Yuge, K. Kurisu, The characteristics of human cranial bone marrow mesenchymal stem cells, *Neurosci. Lett.* 606 (2015) 161–166, <https://doi.org/10.1016/j.neulet.2015.08.056>.
- [2] Y. Hayashi, M. Murakami, R. Kawamura, R. Ishizaka, O. Fukuta, M. Nakashima, CXCL14 and MCP1 are potent trophic factors associated with cell migration and angiogenesis leading to higher regenerative potential of dental pulp side population cells, *Stem Cell Res. Ther.* 6 (2015) 111, <https://doi.org/10.1186/s13287-015-0088-z>.
- [3] Y. Maeda, T. Otsuka, M. Takeda, T. Okazaki, K. Shimizu, M. Kuwabara, M. Hosogai, L. Yuge, T. Mitsuhashi, Transplantation of rat cranial bone-derived mesenchymal stem cells promotes functional recovery in rats with spinal cord injury, *Sci. Rep.* 11 (2021) 21907, <https://doi.org/10.1038/s41598-021-01490-1>.
- [4] K.A. Dunham, A. Siriphorn, S. Chompoopong, C.L. Floyd, Characterization of a graded cervical hemiconfusion spinal cord injury model in adult male rats, *J. Neurotrauma* 27 (2010) 2091–2106, <https://doi.org/10.1089/neu.2010.1424>.
- [5] M. Martinez, J.M. Brezun, L. Bonnier, C. Xerri, A new rating scale for open-field evaluation of behavioral recovery after cervical spinal cord injury in rats, *J. Neurotrauma* 26 (2009) 1043–1053, <https://doi.org/10.1089/neu.2008.0717>.
- [6] J.M. Khor, C.A. Etensohn, Transcription factors of the Alx family: evolutionarily conserved regulators of deuterostome skeletogenesis, *Front. Genet.* 11 (2020), 569314, <https://doi.org/10.3389/fgene.2020.569314>.
- [7] J.L. Nowicki, A.C. Burke, Hox genes and morphological identity: axial versus lateral patterning in the vertebrate mesoderm, *Development* 127 (2000) 4265–4275, <https://doi.org/10.1242/dev.127.19.4265>.
- [8] E.J. Benner, D. Luciano, R. Jo, K. Abdi, P. Paez-Gonzalez, H. Sheng, D.S. Warner, C. Liu, C. Eroglu, C.T. Kuo, Protective astrocytosis from the SVZ niche after injury is controlled by Notch modulator Thbs4, *Nature* 497 (2013) 369–373, <https://doi.org/10.1038/nature12069>.
- [9] H.J. Jeon, J. Park, J.H. Shin, M.S. Chang, Insulin-like growth factor binding protein-6 released from human mesenchymal stem cells confers neuronal protection through IGF-1R-mediated signaling, *Int. J. Mol. Med.* 40 (2017) 1860–1868, <https://doi.org/10.3892/ijmm.2017.3173>.
- [10] J.C. Fleming, M.D. Norenberg, D.A. Ramsay, G.A. Dekaban, A.E. Marcillo, A. D. Saenz, M. Pasquale-Styles, W.D. Dietrich, L.C. Weaver, The cellular inflammatory response in human spinal cords after injury, *Brain* 129 (2006) 3249–3269, <https://doi.org/10.1093/brain/awl296>.
- [11] V. Neirincx, G. Agirman, C. Coste, A. Marquet, V. Dion, B. Rogister, R. Franzen, S. Wislet, Adult bone marrow mesenchymal and neural crest stem cells are chemoattractive and accelerate motor recovery in a mouse model of spinal cord injury, *Stem Cell Res. Ther.* 6 (2015) 211, <https://doi.org/10.1186/s13287-015-0202-2>.
- [12] G. Ren, L. Zhang, X. Zhao, G. Xu, Y. Zhang, A.I. Roberts, R.C. Zhao, Y. Shi, Mesenchymal stem cell-mediated immunosuppression occurs via concerted action of chemokines and nitric oxide, *Cell Stem Cell* 2 (2008) 141–150, <https://doi.org/10.1016/j.stem.2007.11.014>.